JOURNAL OF BACTERIOLOGY, Aug. 2008, p. 5517–5521 Vol. 190, No. 15
0021-9193/08/$08.00+0 doi:10.1128/JB.00407-08

Clusters of Charged Residues at the C Terminus of MotA and N Terminus of MotB Are Important for Function of the *Escherichia coli* Flagellar Motor[▽]

Edan R. Hosking† and Michael D. Manson*

Department of Biology, Texas A&M University, College Station, Texas 77843-3258

Received 22 March 2008/Accepted 28 April 2008

MotA contains a conserved C-terminal cluster of negatively charged residues, and MotB contains a conserved N-terminal cluster of positively charged residues. Charge-altering mutations affecting these residues impair motility but do not diminish Mot protein levels. The motility defects are reversed by second-site mutations targeting the same or partner protein.

The $MotA_4MotB_2$ complex of *Escherichia coli* is the stator of the rotary flagellar motor (5) and the H^+ channel that couples the proton motive force to motility (1, 9, 11–14, 23). At least 11 complexes can be accommodated per motor (17). MotA spans the cytoplasmic membrane four times and has short periplasmic loops between transmembrane segment 1 (TM1) and TM2 and between TM3 and TM4 (3, 21). Large cytoplasmic domains occur between TM2 and TM3 and following TM4. MotB has a cytoplasmic N terminus of 25 residues, a single TM domain, and a periplasmic domain with a conserved peptidoglycan-binding motif (2, 18) that anchors the Mot complex to the cell wall (4, 10).

We asked whether electrostatic interactions between negatively charged residues near the C terminus of MotA and positively charged residues near the N terminus of MotB facilitate formation of the $MotA_4MotB_2$ complex for three reasons. (i) MotB is unstable in the absence of MotA (20), so coinsertion into the membrane and rapid complex assembly might be advantageous. (ii) Translation of *motA* and *motB* is coupled (20). Thus, the initial proximity of the C terminus of MotB and the N terminus of MotB would facilitate their early interaction. (iii) Clusters of charged residues in MotA and MotB are conserved.

Identification of conserved charged residues. Alignment of the N-terminal amino acid sequence of *E. coli* MotB with those from 15 other bacterial species (Fig. 1A) revealed that most species have a cluster of 3 to 6 Arg and Lys residues 12 to 14 residues before the cytoplasmic end of the TM domain. *Rhodobacter sphaeroides* has positively charged residues throughout its N-terminal region. Two to four negatively charged Glu and/or Asp residues typically cluster within 20 residues of the C terminus of MotA. Again, *R. sphaeroides* is an exception.

A stepwise 10-codon deletion analysis (16) showed that removal of codons 271 to 280 of *Salmonella motA* led to a nonmotile phenotype and destabilized the Mot complex. Deletion of residues 11 to 20 of *Salmonella motB* generated slow-motile phenotypes but preserved normal Mot protein levels. Thus, this region of MotB cannot be essential. However, the conservation of charge led us to examine phenotypes associated with charge-altering changes in the ELEE sequence (residues 275 to 278) of MotA and the KRRKAK sequence (residues 12 to 17) of MotB.

Alanine-scanning mutagenesis targeted at charged residues. The Glu codons of MotA were converted to Ala codons in the IPTG (isopropyl-β-D-thiogalactopyranoside)-inducible pHSG575(*motA*$^+$*B*$^+$) plasmid (19). Glu-275, Glu-277, and Glu-278 were substituted together ($MotA_{275\text{-}278A}$). In MotB, Lys-12, Arg-13, and Arg-14 were replaced as one group ($MotB_{12\text{-}14A}$) and Lys-15 and Lys-17 as a second group ($MotB_{15\text{-}17A}$). In the $MotB_{12\text{-}17A}$ variant, all positively charged residues were converted to Ala. The mutant plasmids were introduced into the Δ*motAB* strain MM5000 (19), and the motility of the transformants was assessed (Table 1).

The relative ring diameter of MM5000/$MotA_{275\text{-}278A}B$ cells was 5% that of the wild type. MM5000/$MotAB_{12\text{-}14A}$ cells were completely nonmotile, but the relative ring diameter with MM5000/$MotAB_{15\text{-}17A}$ was 73%. MM5000/$MotAB_{12\text{-}17A}$ cells were completely nonmotile. Wild-type levels of MotA and MotB were detected on immunoblots for all strains (data not shown). Thus, neutralization, by Ala replacement, of the ELEE cluster in MotA or the KRRKAK cluster in MotB severely impaired motility, but the stability of the Mot complex was unaffected.

Site-directed charge-reversing mutations. The ELEE sequence in MotA was converted to KLKK ($MotA_{275\text{-}278K}$), and the KRRKAK sequence was converted to DDDDAD ($MotB_{12\text{-}17D}$). MM5000/$MotA_{275\text{-}278K}B$ and MM5000/$MotAB_{12\text{-}17D}$ cells were completely nonmotile (Table 1). However, the amounts of Mot proteins were normal.

Suppressors of *motA* mutations. Spontaneous suppressors were isolated by inoculating 100-μl aliquots of overnight cultures of MM5000/p$MotA_{275\text{-}278A}B$ or MM5000/p$MotA_{275\text{-}278K}B$ as 6-cm troughs in tryptone semisolid agar. After 36 h at 30°C, six motile flares were found with $MotA_{275\text{-}278A}B$, and three were found with $MotA_{275\text{-}278K}B$ (Table 1). The plasmids were isolated and reintroduced into strain MM5000. All transformants were motile, indicating that the suppressing

* Corresponding author. Mailing address: Department of Biology, Texas A&M University, College Station, TX 77843-3258. Phone: (979) 845-5158. Fax: (979) 845-2891. E-mail: mike@mail.bio.tamu.edu.

† Present address: Department of Molecular, Cellular and Developmental Biology, University of Michigan, Ann Arbor, MI 48109.

▽ Published ahead of print on 9 May 2008.

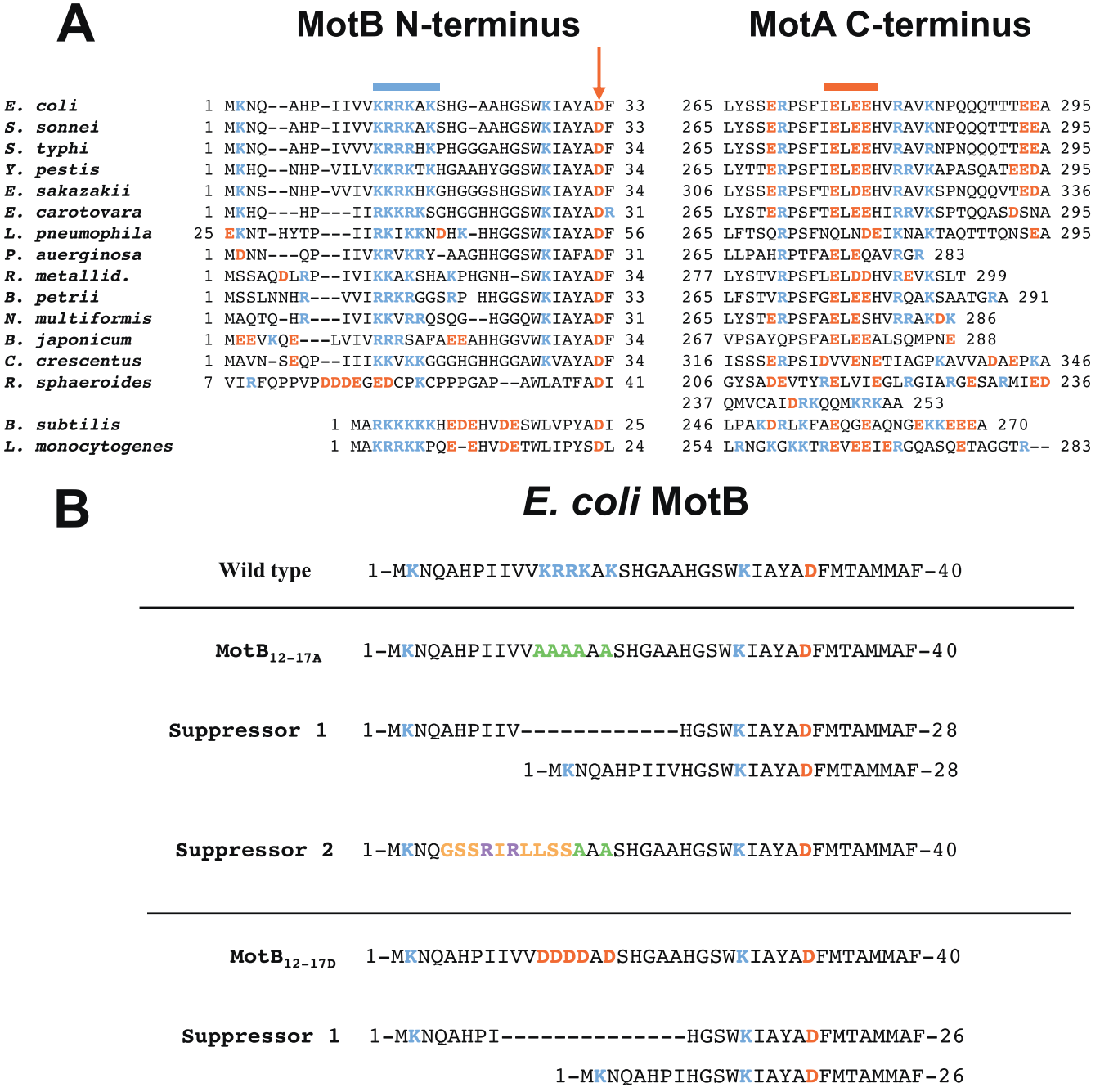

FIG. 1. (A) Alignment of the N-terminal amino acid sequences of MotB and C-terminal amino acid sequences of MotA for 16 diverse bacterial species. The numbers indicate the positions of the first and last residues in the sequence. Positively charged residues are highlighted blue, and negatively charged residues are highlighted red. The blue and red lines identify the positions of the clusters of positively charged residues in MotB and of negatively charged residues in MotA, respectively. The beginning of the TM helix of MotB is underlined in black, and the absolutely conserved Asp residue that is protonated and deprotonated during proton flow (22) is indicated by the vertical red arrow. The sequences are from *Escherichia coli*, *Shigella sonnei*, *Salmonella enterica* serovar Typhi, *Yersinia pestis*, *Enterobacter sakazaki*, *Erwinia carotovara*, *Legionella pneumophila*, *Pseudomonas aeruginosa*, *Ralstonia metallidurans*, *Bordetella petrii*, *Nitrosolobus multiformis*, *Bradyrhizobium japonicum*, *Caulobacter crescentus*, *Rhodobacter sphaeroides*, *Bacillus subtilis*, and *Listeria monocytogenes*. (B) Sequences of the suppressors of the $MotB_{12\text{-}17A}$ and $MotB_{12\text{-}17D}$ mutations. The top sequence is the first 40 residues of *E. coli* wild-type MotB. Basic residues are shown in blue, and negatively charged residues are shown in red. The second sequence is for the $MotB_{12\text{-}17A}$ mutant. The introduced Ala residues are shown in green. The third and fourth lines are the first suppressor of $MotB_{12\text{-}17A}$ (removal of residues 11 to 22). The fifth line is the second suppressor of the $MotB_{12\text{-}17A}$ mutant (a +8 frameshift mutation in codon 5 and a −8 frameshift mutation in codons 12 to 14 of *motB*). Six of the altered residues are shown in orange, whereas the positively charged Arg residues are shown in purple. The sixth line is the $MotB_{12\text{-}17D}$ mutant. The introduced Asp residues are shown in red. The seventh and eighth lines show the suppressor of the $MotB_{12\text{-}17D}$ mutant (removal of residues 9 to 22).

TABLE 1. Motility of mutants and suppressed mutants obtained in this study

Mutation[a]	Sequence change[b]	Suppressor[c]	Motility (%)[d]
None (wild-type)	None	None	100 ± 5
$MotA_{275\text{-}278A}$	ELEE→ALAA	None	5
		MotA L63S	71 ± 5
		MotA R66H	71 ± 5
		MotA F95L	75 ± 2
		MotA G136V	77 ± 7
		MotA E149A	70 ± 1
		MotB R237H	39 ± 3
$MotA_{275\text{-}278K}$	ELEE→KLKK	None	0
		MotA E142K (twice)	35 ± 3
		MotA E144K	19 ± 2
$MotB_{12\text{-}14A}$	KRK→AAA	None	0
		MotA M237I	66 ± 4
		MotA Q239R	58 ± 4
		MotA L246R	63 ± 6
		MotB H138Y (twice)	60 ± 5
		MotB I152V	62 ± 5
		MotB R173C	38 ± 5
		Chromosomal	43 ± 5
$MotB_{15\text{-}17A}$	KAK→AAA	None	73
$MotB_{12\text{-}17A}$	KRRKAK→AAAAA	None	0
		Δ*motB* codons 11 to 22 (seven times)	26 ± 3
		motB double frameshift mutation, +8 (codon 5) and −8 (codon 15)	54 ± 4
$MotB_{12\text{-}17D}$	KRRKAK→DDDDAD	None	0
		Δ*motB* codons 9 to 22	63 ± 7

[a] Name of mutation as it appears in the text.
[b] Residue substitutions made.
[c] Nature of the suppressing mutation, if any.
[d] Relative chemotactic ring diameter in tryptone (15) semisolid agar (0.325%) incubated at 30°C compared to that for strain MM5000(Δ*motAB*) carrying wild-type plasmid pHSG575($motA^+B^+$). The standard deviation of the mean is also given.

mutations were plasmid borne. Each plasmid contained a second-site mutation.

The five *motA* suppressors of $MotA_{275\text{-}278A}B$ generated the residue changes L63S, R66H, F95L, G136V, and E149A and restored 70% of the relative ring diameter (Table 1). The *motB* suppressor created the change R237H and supported a 40% relative ring diameter. The E142K suppressor of $MotA_{275\text{-}278K}B$, found twice, restored a relative ring diameter of 35%. The E144K suppressor led to a relative ring diameter of 19%. Wild-type levels of Mot proteins were present in each case, demonstrating that motility was not restored by increased Mot protein production.

Suppressors of *motB* mutations. Eight motile flares were isolated from $MotAB_{12\text{-}14A}$. Seven plasmids restored motility when reintroduced into strain MM5000. Three suppressors (M237I, Q239R, and L246R) targeted MotA, and four (H138Y [twice], I152V, and R173C) targeted MotB (Table 1). The eighth plasmid did not restore motility and contained no second-site mutation in plasmid-borne *mot* genes. Thus, the suppressing mutation was chromosomal.

The *motA* suppressors restored relative ring diameters of 60% (Table 1), as did the H138Y and I152V substitutions in MotB. The R173C MotB substitution supported a relative ring diameter of 38%, and the chromosomal suppressor was 43% efficient. All suppressed mutants had wild-type Mot protein levels.

The $MotAB_{12\text{-}17A}$ mutant gave rise to eight plasmid-borne suppressors. Seven contained a deletion of *motB* codons 11 to 22 (Fig. 1B). The eighth had a double frameshift mutation that inserted eight bases between the first and second bases of codon 5 and deleted codons 12 and 13 and the first two bases of codon 14. These changes altered the sequence of residues 5 through 14 and introduced Arg residues at positions 8 and 10 (Fig. 1B). The relative swarm diameters for strains expressing $MotAB_{\Delta 11\text{-}22}$ and $MotAB_{8R/10R}$ were 27% and 54%, respectively (Table 1). One suppressor was found for $MotAB_{12\text{-}17D}$, a deletion of MotB codons 9 to 22 (Fig. 1B). The relative ring diameter of the suppressed mutant was 62% (Table 1). All suppressed mutants had wild-type Mot protein levels. The phenotypes associated with these deletions, which confer a slow-motile phenotype without noticeably affecting Mot complex stability, resemble the phenotype of a strain in which residues 11 to 20 in *Salmonella* MotB were removed (16).

Conclusion. We falsified the hypothesis that electrostatic interactions between clusters of charged residues at the C terminus of MotA and the N terminus of MotB contribute significantly to formation of stable Mot protein complexes.

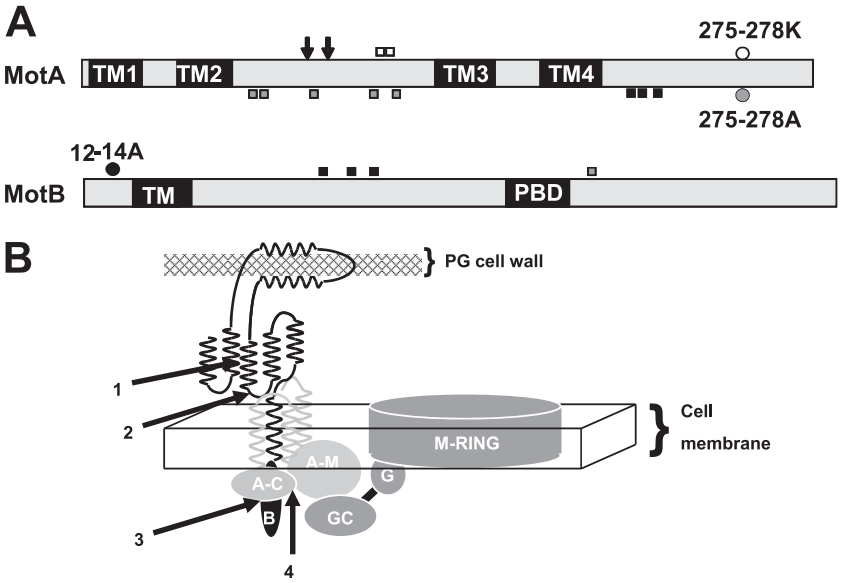

FIG. 2. (A) Positions of the point mutations that suppress charge-altering residue changes in MotA and MotB. Mutations are indicated by name, and their approximate locations within the protein are indicated by circles. The locations of the corresponding suppressors are highlighted by squares, each with the same color as the original mutation. The suppressors of $MotA_{275\text{-}278K}$ are E142K and E144K; the suppressors of $MotA_{275\text{-}278A}$ are L63S, R66H, F95L, G136V, and E149A in MotA and R237H in MotB; and the suppressors of $MotB_{11\text{-}14A}$ are M237I, Q239R, and L246R in MotA and H138Y, I152V, and R173C in MotB. The locations of the TM domains of MotA and MotB, and the proposed peptidoglycan-binding domain (PBD) of MotB, are labeled. The positions of residues Arg-90 and Glu-98 of MotA, which interact electrostatically with FliG (21), are indicated by the two downward-facing arrows. (B) Schematic of possible interactions within the Mot complex. The components are not drawn to scale. MotA is medium gray, Mot B is black, and rotor elements are dark gray. TM1 of MotA is eliminated for clarity. The N-terminal extension of MotB is shown as a black oval, labeled B. The N-terminal domain of FliG that associates with the M ring is labeled G, and the C-terminal motility domain of FliG is labeled GC. The two predicted α helices of the peptidoglycan-binding domain are shown in contact with the cell wall, and the cytoplasmic domain of MotA between TM2 and TM3, labeled AM, is shown in contact with the motility domain of FliG. Possible interactions suggested by this and earlier (6–8) studies are as follows: (1) between the C-terminal region of MotB that contains Arg-237 and the two predicted helices containing MotB residues His-138, Ile-152, and Arg-173; (2) between the helices containing MotB residues His-138, Ile-152, and Arg-173 and the TM3-TM4 periplasmic loop; (3) between the cytoplasmic N terminus of MotA and the C-terminal cytoplasmic domain of MotA that follows TM4, labeled AC; and (4) between the AM and AC domains of MotA. We note that neither the original mutations nor their suppressors must be located at these sites; residue changes could affect the interaction indirectly from a distance.

However, neutralizing or reversing the charges of residues Glu-275, Glu-277, and Glu-278 of MotA or residues Lys-12, Arg-13, Arg-14, Lys-15, and Lys-17 of MotB impaired motility (Table 1).

Second-site mutations in *motA* that suppress motility defects of $MotA_{275\text{-}278A}B$ (L63S, R66H, F95L, G136V, and E149A) or $MotA_{275\text{-}278K}B$ (E142K and E144K) target the cytoplasmic domain between TM2 and TM3 of MotA (Fig. 2A). Two changes are N terminal to the Arg-90 and Glu-98 residues, which interact electrostatically with opposite charges in FliG (22). Four more changes are C terminal to Arg-90 and Glu-98, and the F95L substitution is located between them. Although we did not check for allele specificity, the E142K and E144K suppressors of $MotA_{275\text{-}278D}$ affect the same region of MotA as the G136V and E149A suppressors of $MotA_{275\text{-}278A}$. The locations of the suppressing mutations suggest that they modify the interaction between the two cytoplasmic domains of MotA to align Arg-90 and Glu-98 properly with FliG.

Three of the $MotB_{12\text{-}14A}$ suppressors altered residues in the C-terminal domain of MotA (M237I, Q239R, and L246R), upstream of the ELEE sequence (Fig. 2A). There is no overlap in the locations of the $MotA_{275\text{-}278A}$/$MotA_{275\text{-}278K}$ and $MotB_{12\text{-}14A}$ suppressors, suggesting that these mutations perturb different protein-protein interactions that require different corrective measures.

The MotB suppressor of $MotA_{275\text{-}278A}$, R237H, alters a residue located 10 residues after the peptidoglycan-binding motif of MotB (4, 10), whereas the three MotB suppressors of $MotB_{12\text{-}14A}$ (H138Y, I152V, and R173C) alter residues between the MotB TM domain and the peptidoglycan-binding site (Fig. 2). This result reinforces the conclusion (6–8) that proper positioning of the Mot complex relative to the motor requires a defined conformation of the MotB periplasmic domain (6–8). The H138Y substitution in MotB suppresses both $MotAB_{12\text{-}14A}$ and the V207M substitution in TM4 of MotA (7). The chromosomal suppressor of $MotAB_{12\text{-}14A}$ may lie in *fliG* and restore proper stator/FliG alignment (8).

All suppressors of the $MotB_{12\text{-}17A}$ and $MotB_{12\text{-}17D}$ mutations delete the mutated region or introduce a double frameshift mutation that alters the amino acid sequence over the mutated region (Fig. 1B). In each case, neutral or negatively charged residues introduced at positions 12 to 17 are deleted or altered. The frameshift suppressor introduces two positively charged Arg residues. This region cannot be crucial for MotB function, since it can be deleted without destroying motility or lowering MotB levels (16; this study). However, stretches of

neutral Ala or negatively charged Asp residues must have a strongly deleterious effect on the conformation of the Mot complex. The effect is drastic enough that suppression through point mutations is improbable.

The interactions that we identified are summarized in Fig. 2B. These are not the only interactions possible. However, we hope that the mutations that we have analyzed, and the suppressors that we have isolated, will help elucidate the mechanism of Mot complex/FliG interaction once structural models are available for all components.

We thank Tim Braun and David Blair for providing antisera to Mot proteins. The manuscript was thoroughly proofread by Lily Z. K. Bartoszek.

The initial research was supported by Army Research Office grant DAAG55-97-1-0380 to M.D.M. The Bartoszek Fund for Basic Biological Science provided financial and emotional support for the later stages of the work.

REFERENCES

1. **Blair, D. F., and H. C. Berg.** 1990. The MotA protein of *E. coli* is a proton-conducting component of the flagellar motor. Cell **60:**439–449.
2. **Chun, S. Y., and J. S. Parkinson.** 1988. Bacterial motility: membrane topology of the *Escherichia coli* MotB protein. Science **239:**276–278.
3. **Dean, G. E., R. M. Macnab, J. Stader, P. Matsumura, and C. Burke.** 1984. Gene sequence and predicted amino acid sequence of the MotA protein, a membrane-associated protein required for flagellar rotation in *Escherichia coli*. J. Bacteriol. **159:**991–999.
4. **De Mot, R., and J. Vanderleyden.** 1994. The C-terminal sequence conservation between OmpA-related outer membrane proteins MotB suggests a common function in both Gram-positive and Gram-negative bacteria, possibly in the interaction of these domains with peptidoglycan. Mol. Microbiol. **12:**333–334.
5. **Francis, N. R., V. M. Irikura, S. Yamaguchi, D. J. DeRosier, and R. M. Macnab.** 1992. Localization of the *Salmonella typhimurium* flagellar switch protein FliG to the cytoplasmic M-ring face of the basal body. Proc. Natl. Acad. Sci. USA **89:**6304–6308.
6. **Garza, A. G., R. Biran, J. A. Wohlschlegel, and M. D. Manson.** 1996. Mutations in *motB* suppressible by changes in stator or rotor components of the bacterial flagellar motor. J. Mol. Biol. **258:**270–285.
7. **Garza, A. G., P. A. Bronstein, P. A. Valdez, L. W. Harris-Haller, and M. D. Manson.** 1996. Extragenic suppression of *motA* missense mutations of *Escherichia coli*. J. Bacteriol. **178:**6116–6122.
8. **Garza, A. G., L. W. Harris-Haller, R. A. Stoebner, and M. D. Manson.** 1995. Motility protein interactions in the bacterial flagellar motor. Proc. Natl. Acad. Sci. USA **92:**1970–1974.
9. **Glagolev, A. N., and V. P. Skulachev.** 1978. The proton pump is a molecular engine of motile bacteria. Nature **272:**280–282.
10. **Koebnik, R.** 1995. Proposal for a peptidoglycan-associating alpha-helical motif in the C-terminal regions of some bacterial cell-surface proteins. Mol. Microbiol. **16:**1269–1270.
11. **Kojima, S., and D. F. Blair.** 2004. Purification and solubilization of the MotA/MotB complex of *Escherichia coli*. Biochemistry **43:**26–34.
12. **Kojima, S., and D. F. Blair.** 2001. Conformational change in the stator of the bacterial flagellar motor. Biochemistry **40:**13041–13050.
13. **Manson, M. D., P. Tedesco, H. C. Berg, F. M. Harold, and C. van der Drift.** 1977. A protonmotive force drives bacterial flagella. Proc. Natl. Acad. Sci. USA **74:**3060–3064.
14. **Matsura, S., J.-I. Shioi, and Y. Imae.** 1977. Motility in *Bacillus subtilis* driven by an artificial protonmotive force. FEBS Lett. **82:**187–190.
15. **Miller, J. H.** 1972. Experiments in Molecular Genetics. Cold Spring Harbor Laboratory, Cold Spring Harbor, NY.
16. **Muramoto, K., and R. M. Macnab.** 1998. Deletion analysis of MotA and MotB, force-generating units in the flagellar motor of *Salmonella*. Mol. Microbiol. **29:**1191–1202.
17. **Reid, S. W., M.C. Leake, J. H. Chandler, C. J. Lo, J. P. Armitage, and R. M. Berry.** 2006. The maximum number of torque-generating units in the flagellar motor of *Escherichia coli* is at least 11. Proc. Natl. Acad. Sci. USA **103:**8066–8071.
18. **Stader, J., P. Matsumura, D. Vacante, G. E. Dean, and R. M. Macnab.** 1986. Nucleotide sequence of the *Escherichia coli motB* gene and site-limited incorporation of its product into the cytoplasmic membrane. J. Bacteriol. **166:**244–252.
19. **Van Way, S. M., E. R. Hosking, T. F. Braun, and M. D. Manson.** 2000. Mot protein assembly into the bacterial flagellum: a model based on mutational analysis of the *motB* gene. J. Mol. Biol. **297:**7–24.
20. **Wilson, M. L., and R. M. Macnab.** 1990. Co-overproduction and localization of the *Escherichia coli* motility proteins MotA and MotB. J. Bacteriol. **172:**3932–3939.
21. **Zhou, J., R. T. Fazzio, and D. F. Blair.** 1995. Membrane topology of the MotA protein of Escherichia coli. J. Mol. Biol. **251:**237–242.
22. **Zhou, J., S. A. Lloyd, and D. F. Blair.** 1998. Electrostatic interactions between rotor and stator in the bacterial flagellar motor. Proc. Natl. Acad. Sci. USA **95:**6436–6441.
23. **Zhou, J., L. L. Sharp, H. L. Tang, S. A. Lloyd, S. Billings, T. F. Braun, and D. F. Blair.** 1998. Function of protonatable residues in the flagellar motor of *Escherichia coli*: a critical role for Asp 32 of MotB. J. Bacteriol. **180:**2729–2735.